

A novel soluble ACE2 protein provides lung and kidney protection in mice susceptible to lethal SARS-CoV-2 infection

SUPPLEMENT

Authors: Luise Hassler¹, Jan Wysocki¹, Ian Gelarden¹, Isha Sharma¹, Anastasia Tomatsidou^{2,3}, Minghao Ye¹, Haley Gula^{2,3}, Vlad Nicolescu^{2,3}, Glenn Randall^{2,3}, Sergii Pshenychnyi⁴, Nigar Khurram¹, Yashpal Kanwar¹, Dominique Missiakas³, Jack Henkin⁵, Anjana Yeldandi¹, and Daniel Batlle^{1*}

Affiliations:

¹ Division of Nephrology/Hypertension, Department of Medicine and the Department of Pathology, Northwestern University, Feinberg School of Medicine, Chicago, Illinois

² Department of Microbiology, The University of Chicago, Chicago, Illinois

³ Ricketts Regional Biocontainment Laboratory, University of Chicago, Lemont, Illinois

⁴ Recombinant Protein Production Core, Northwestern University, Evanston, IL, USA

⁵ Center for Developmental Therapeutics, Northwestern University, Evanston, IL, USA

*corresponding author

Preprint: DOI 10.1101/2021.03.12.435191

Correspondence:

Dr. Daniel Batlle

Division of Nephrology and Hypertension, Department of Medicine

Northwestern University, The Feinberg School of Medicine

320 E Superior, Tarry 14-727, Chicago, IL 60611

Email: d-batlle@northwestern.edu

Table of content:

- Supplementary figures E1-E9
- Table 1

Fig E1.

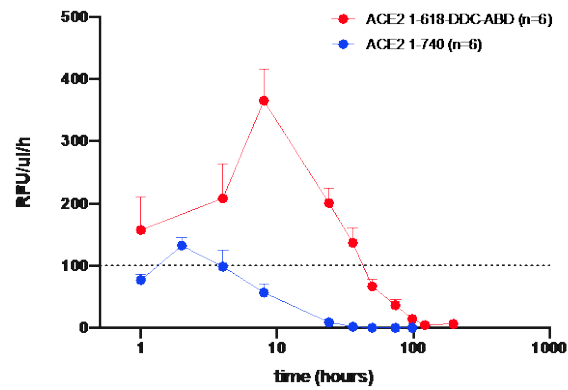
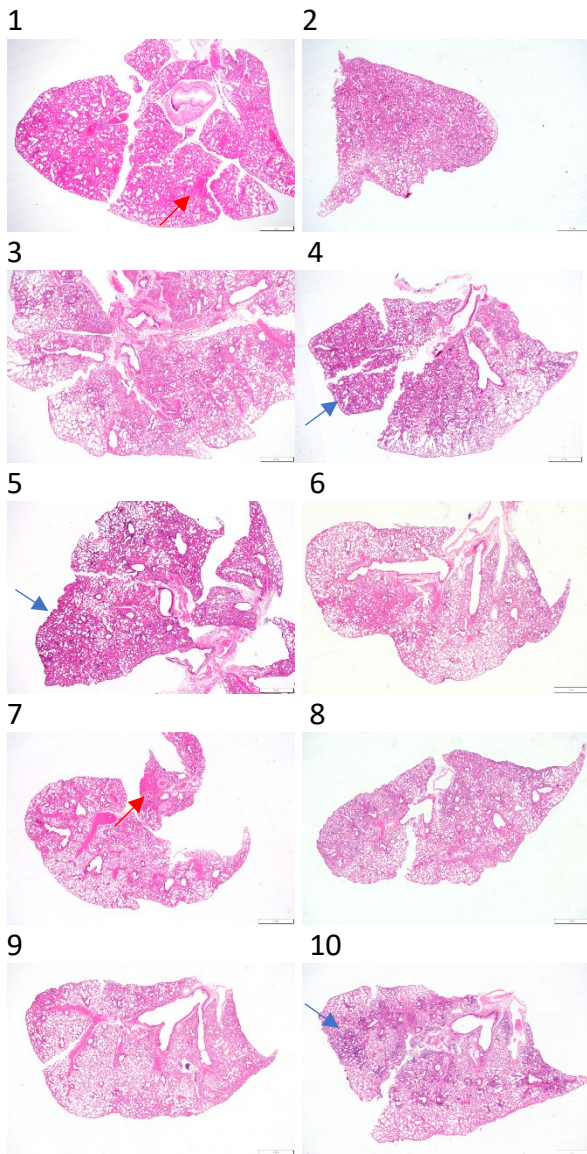


Fig E1. Pharmacokinetics of ACE2 1-618-DDC-ABD and ACE2 1-740.

The ACE2 1-618-DDC-ABD (red) variant resulted in higher plasma ACE2 activity than native soluble ACE2 1-740 (blue) post intraperitoneal injection. Moreover, after native ACE2 1-740 administration, plasma ACE2 activity decreased already after 8 hours post injection whereas ACE2 618-DDC-ABD resulted in markedly increased duration of action as shown by substantial plasma ACE2 activity at 72 hours.

Fig. E2.

PBS:



ACE2 1-618-DDC-ABD:

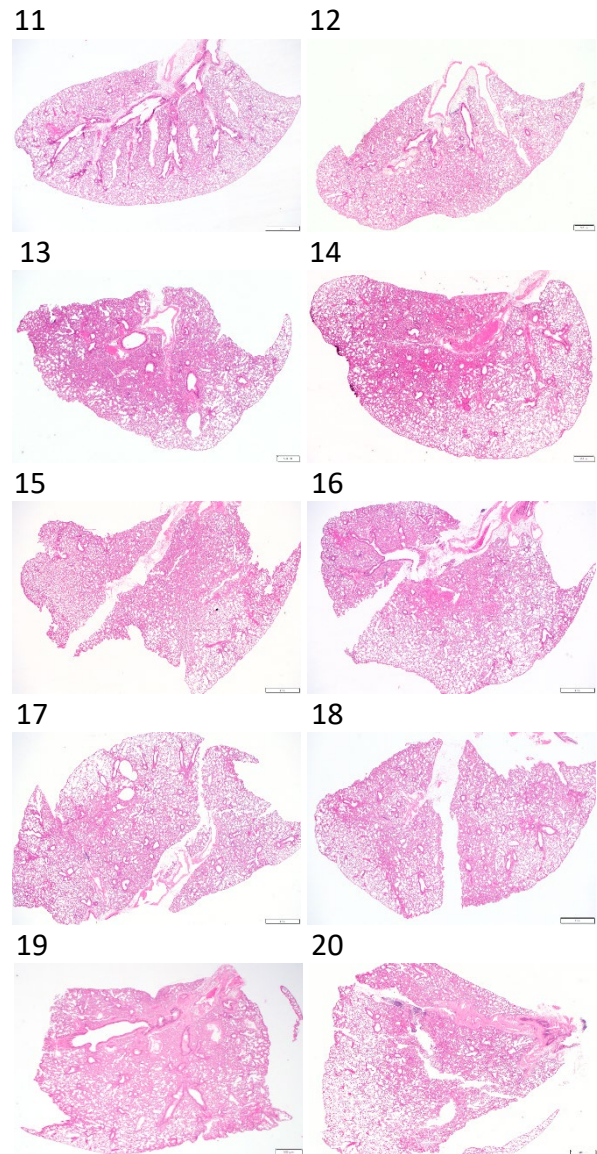
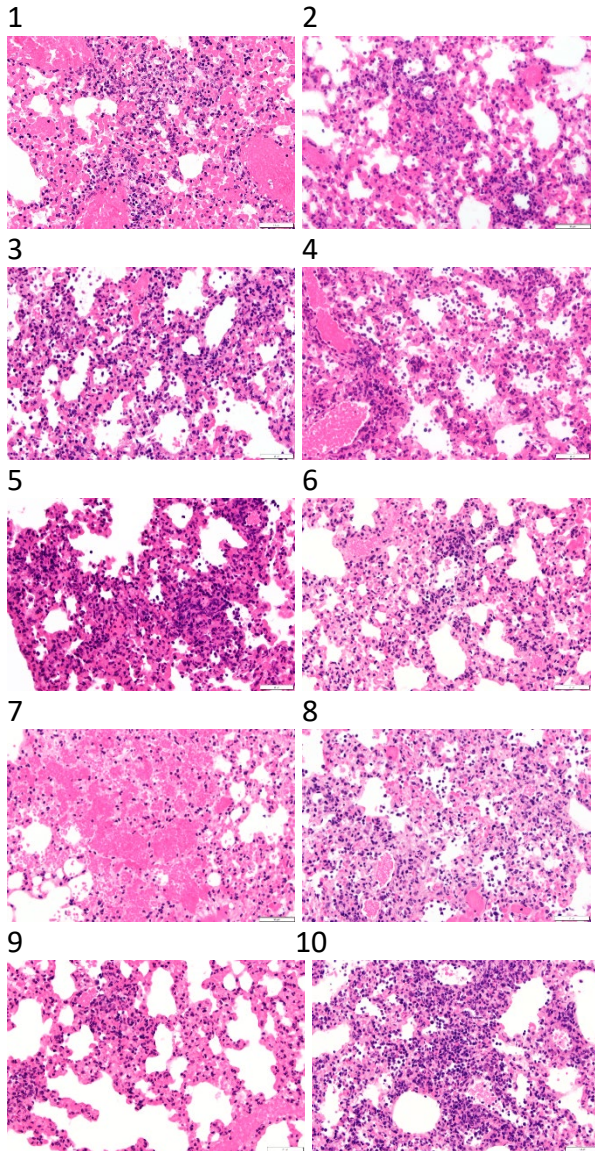


Figure E2. Histopathology of lungs stained with hematoxylin and eosin, presented are low power views X20.

An overview of sections of one lung from SARS-CoV-2 infected animals untreated (n=10, left panel) or treated with ACE2 1-618-DDC-ABD (n=10, right panel). Overall, lungs of all untreated animals show extensive perivascular and interstitial basophilic mononuclear infiltrates (blue arrows show representative foci) and eosinophilic alveolar hemorrhage (red arrows show representative foci) compared to treated animals with much less apparent involvement and in some cases appear essentially normal at low power (cases 11, 12, 15, 17, 18, and 19). Cases 1-10 (left) are untreated and sacrificed at day 6/7 post viral inoculation, cases 11-14 (right) are treated with ACE2 1-618-DDC-ABD and sacrificed on day 6, cases 17-20 (right) are also treated and were sacrificed on day 14 post viral inoculation. Scale bars = 1mm.

Fig. E3.

PBS:



ACE2 1-618-DDC-ABD:

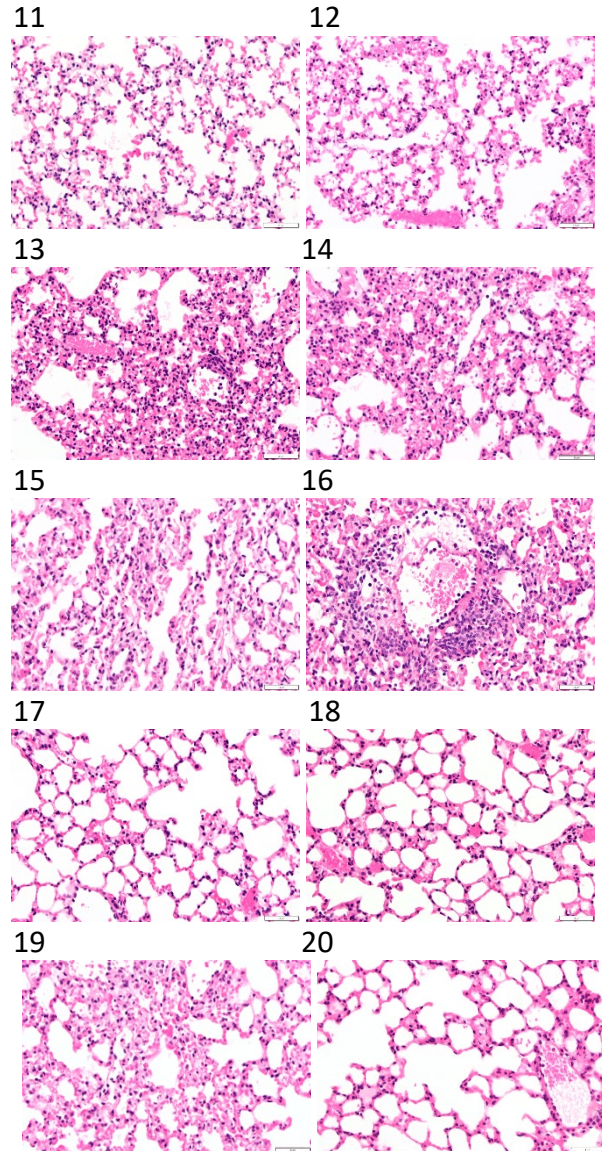
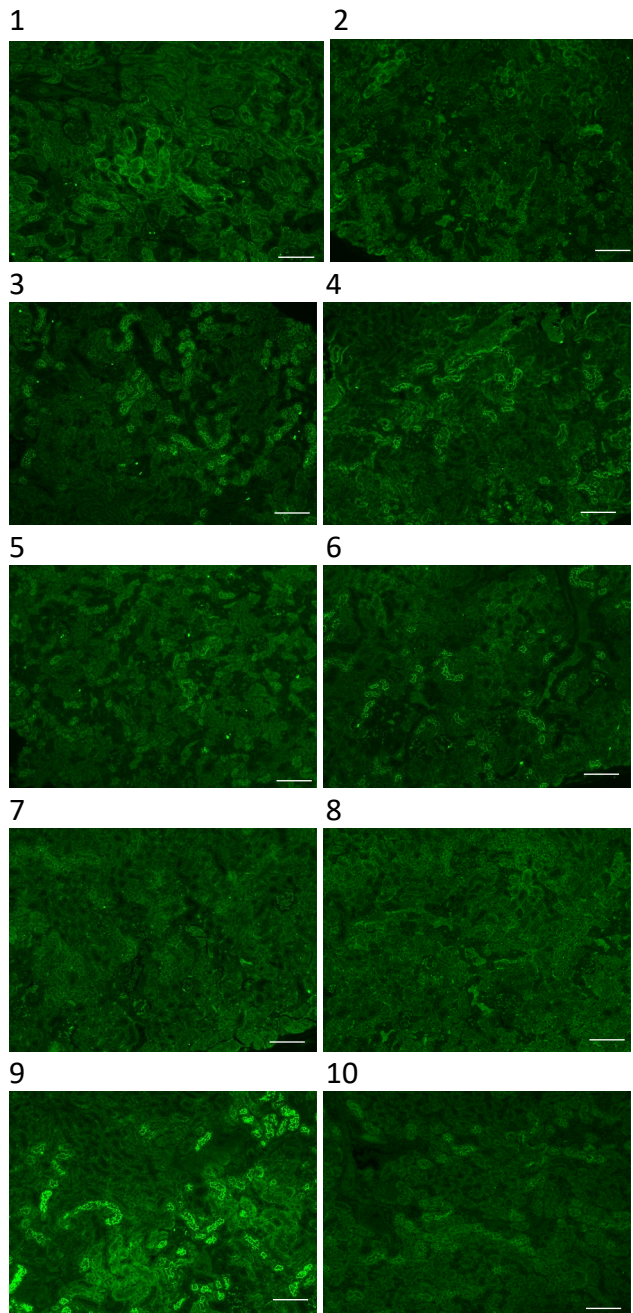


Figure E3. Histopathology in lungs stained with hematoxylin and eosin, presented are high power views X400. Examination of lungs showed extensive alveolar damage with hemorrhage, perivascular and interstitial infiltrates, in all untreated animals (left panels). In sharp contrast, the lungs of animals treated with ACE2 1-618-DDC-ABD (right panels) show less alveolar damage, with many cases appearing largely normal (11, 12, 15, 17, 18, 19, and 20). Cases 1-10 (left) are untreated and sacrificed at day 6/7 post viral inoculation, cases 11-14 (right) are treated with ACE2 1-618-DDC-ABD and sacrificed on day 6, cases 17-20 (right) are also treated and were sacrificed on day 14 post viral inoculation. Scale bars = 50µm.

Fig. E4.

PBS:



ACE2 1-618-DDC-ABD:

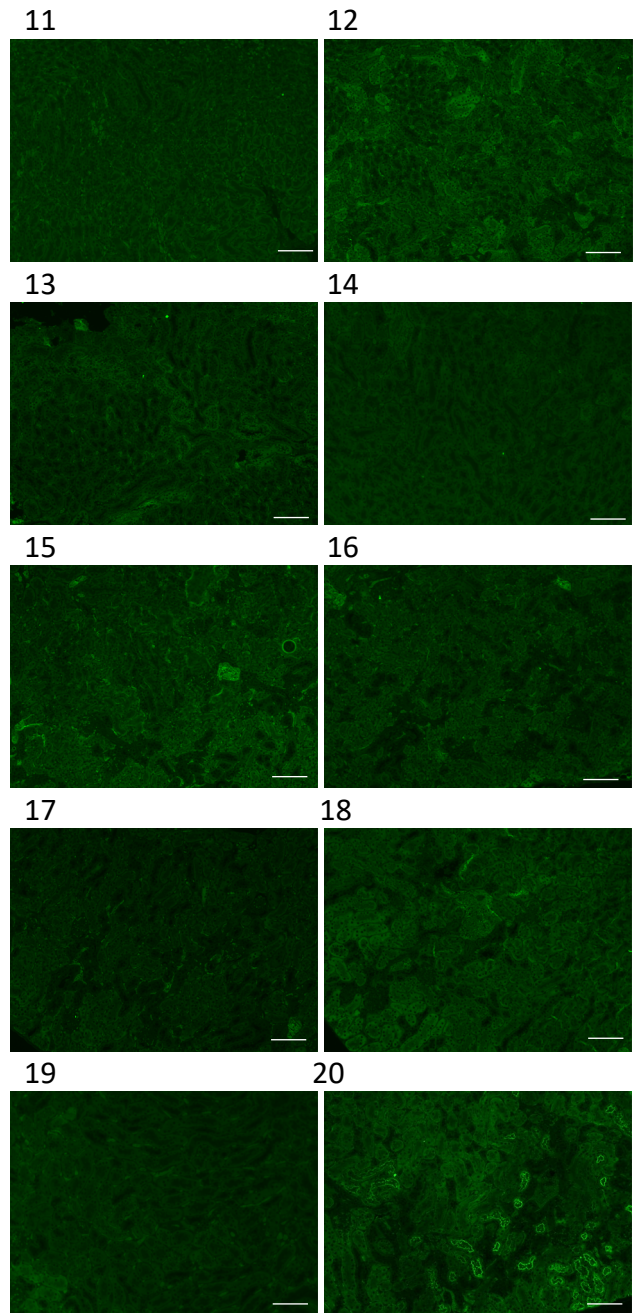


Figure E4. Kidneys stained for NGAL, presented are low power views X100.

Kidneys of infected, PBS-treated mice displayed NGAL staining in the proximal tubule brush border in all cases with varying staining intensity (left panels, cases 1-10). Kidneys of infected, ACE2-1-618-DDC-ABD treated mice, by contrast, showed no staining (right panels, cases 11-20), except for very light staining in case 13 (scored as 0.5, fig 5D) and case 20 (scored as 2.0, fig 5D). Cases 1-10 (left) are untreated and sacrificed at day 6/7 post viral inoculation, cases 11-14 (right) are treated with ACE2 1-618-DDC-ABD and sacrificed on day 6, cases 17-20 (right) are also treated and were sacrificed on day 14 post viral inoculation. Scale bars = 100µm.

Fig. E5.

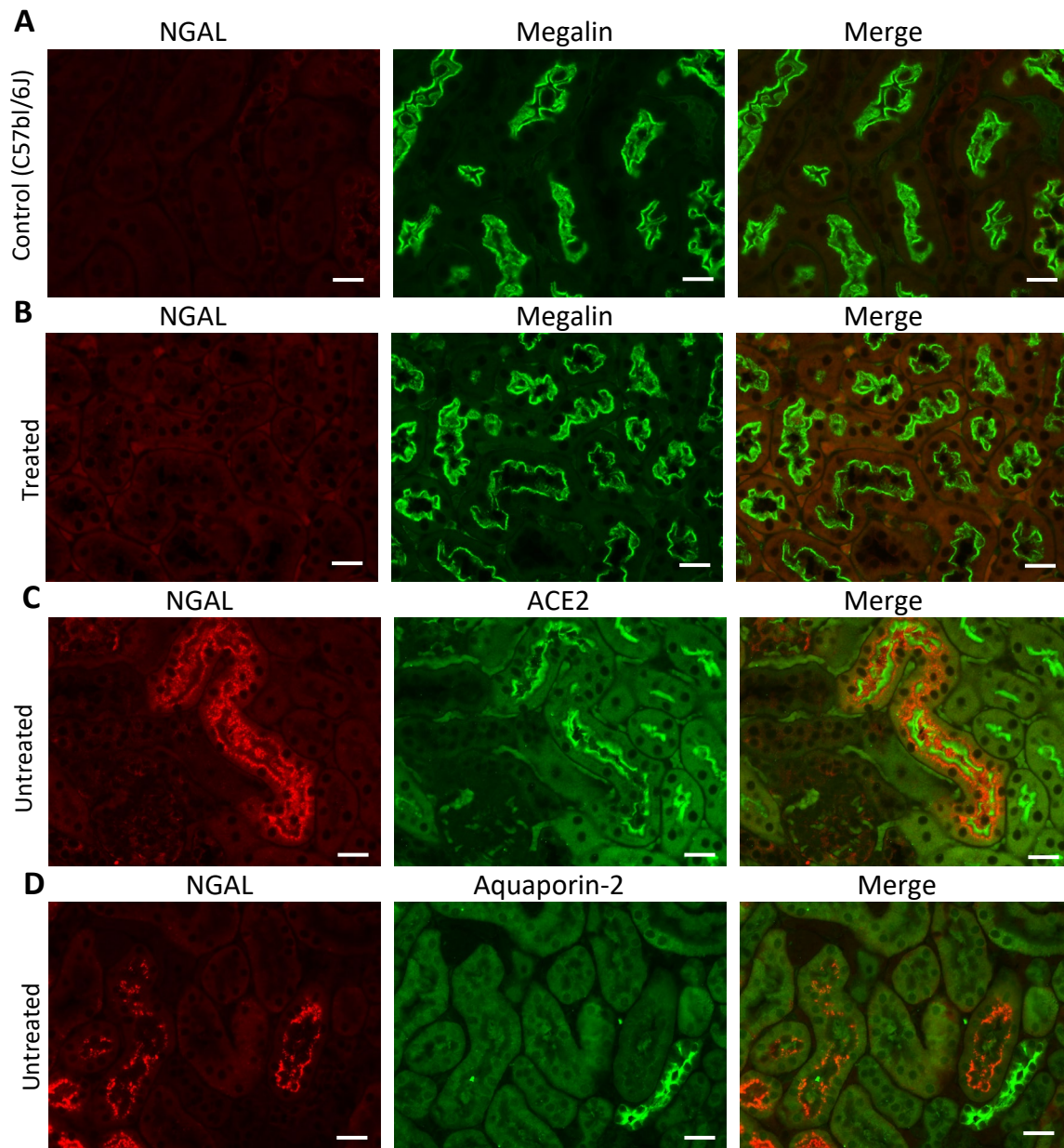
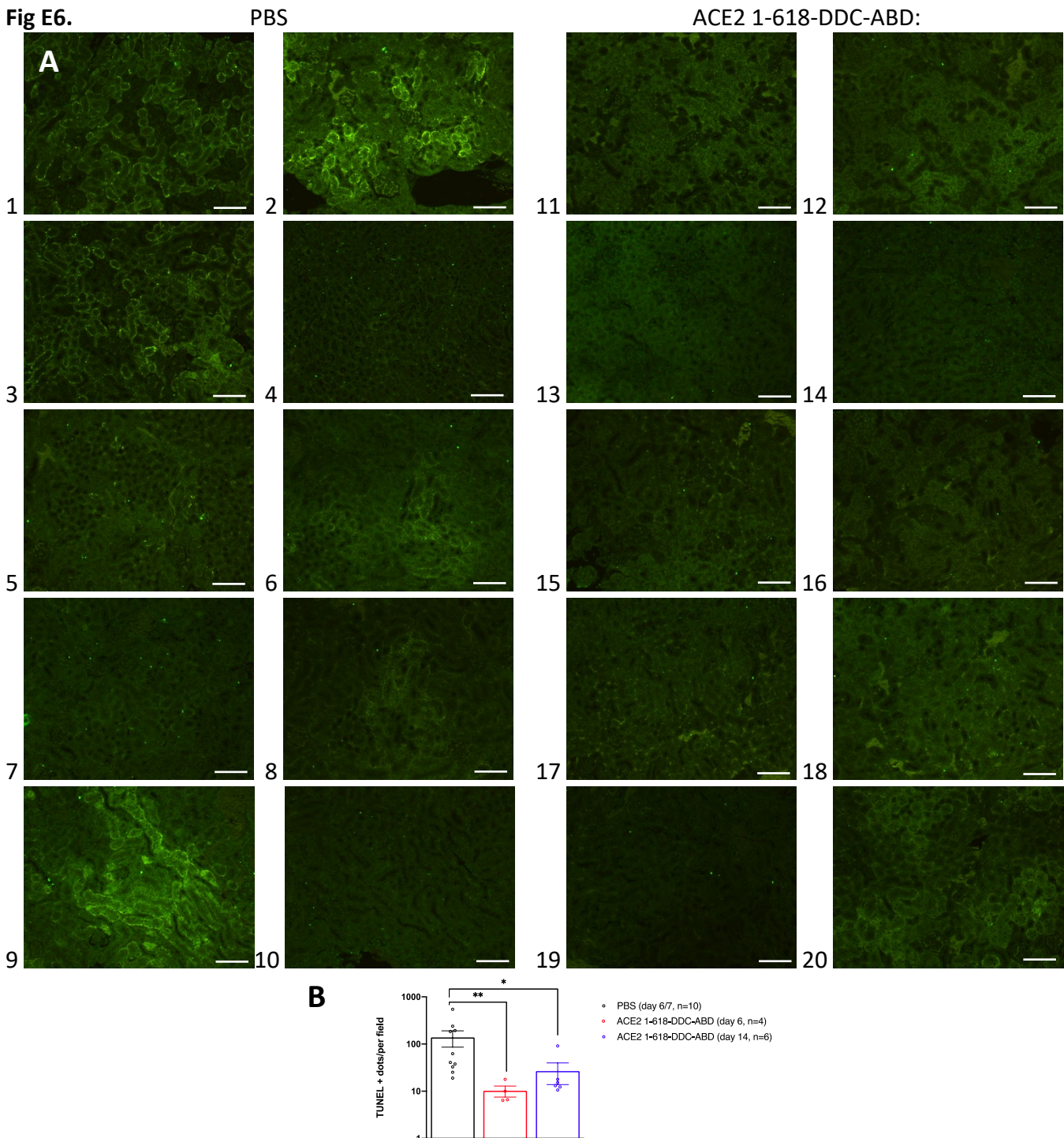


Figure E5. Representative patterns of NGAL co-staining with megalin, ACE2 or aquaporin 2.

Panel A, B. In the kidney of an uninfected control mouse of the same background as the k18hACE2 mice (C57BL/6J) (A) or an infected k18hACE2 mouse that received ACE2 1-618-DDC-ABD (B), NGAL staining (red) was non-detectable. Megalin (green) was used as a marker of the proximal tubule; since NGAL is not present there was no co-localization (A, B).

Panel C, D. In the kidney of an infected k18hACE2 mouse that was untreated, NGAL staining co-localized with ACE2 as a proximal tubular marker (C), but not with Aquaporin 2, a marker of the collecting tubule (D). Scale bar = 20um, magnification: 400x.

Fig E6.**Figure E6. Kidneys stained with the TUNEL assay kit, presented are low power views X200.**

Panel A. Kidneys of infected, PBS-treated mice display a high number of apoptotic nuclei and diffusely spread smaller TUNEL positive bodies in proximal tubules (left). In ACE2 1-618-DDC-ABD treated animals, by contrast apoptotic nuclei were less frequent, only case 20 showed smaller TUNEL positive bodies. Cases 1-10 (left) are untreated and sacrificed at day 6/7 post viral inoculation, cases 11-14 (right) received ACE2 1-618-DDC-ABD and were sacrificed on day 6, cases 17-20 (right) also received ACE2 1-618-DDC-ABD and were sacrificed on day 14 post viral inoculation. Scale bars = 50µm. **Panel B.** The number of TUNEL positive dots per field is higher in the PBS-group (n=10, 138 ± 52) than in the ACE2 1-618-DDC-ABD-groups at day 6 (n=4, 10 ± 2, p=0.0023) or 14 (n=6, 26 ± 12, p=0.0414, calculated using Kruskal-Wallis-test, followed by post-hoc Dunn's multiple comparisons test). To search for only nuclear localization co-localization studies were done (**fig E7, 8**).

Fig. E7.

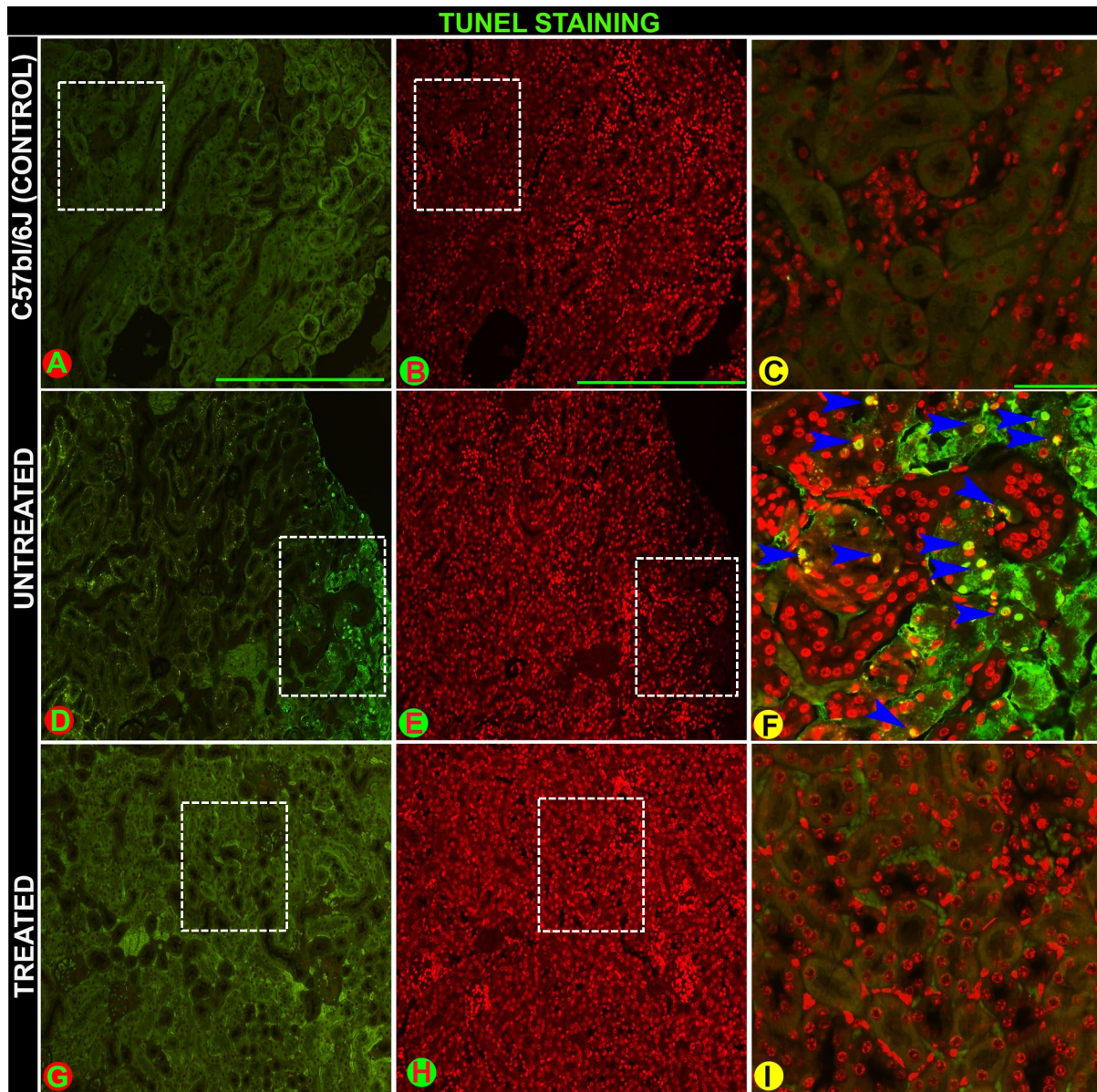


Figure E7. TUNEL-TO-PRO™-3 iodide co-staining in kidneys of k18hACE2-mice infected with SARS-CoV-2. **Panels A-C.** In a kidney from an uninfected control mouse of the same background (C57bl/6J) as the transgenic k18hACE2 mice, there is no evidence of apoptosis as assessed by the absence of TUNEL-staining (**A**, green). TO-PRO™-3 iodide staining (red) was used to highlight nuclei (**B**). In the absence of positive TUNEL-staining (**A**), the merged image (**C**) does not show any apoptotic cells. **Panels D-F.** Positive TUNEL staining (green) was observed in the cortical region of the kidney of an untreated, infected k18hACE2 mouse (**D**). The nuclei with yellow coloration represent co-localization of apoptotic nuclei and the nuclear dye (**F**, blue arrowheads). **Panels G-I.** The kidneys of an infected mouse that received ACE2 1-618-DDC-ABD, show no TUNEL positive staining (**G**) and thus also no co-localization with TO-PRO™-3 red dye (**I**). Panel A, B scale bar-100 μ m, Panel C scale bar-50 μ m. Magnification: 200x.

Fig E8.

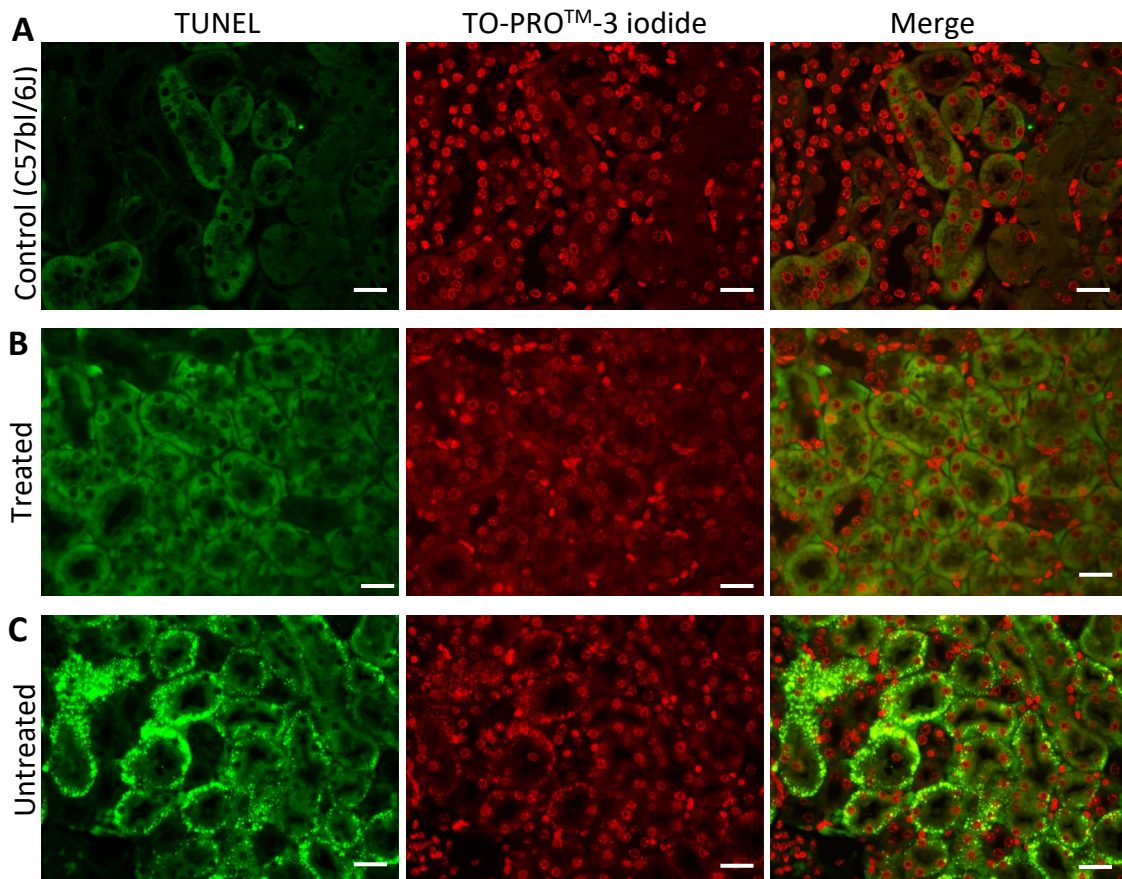


Figure E8. TUNEL-TO-PRO™-3 iodide co-staining in kidneys of k18hACE2-mice infected with SARS-CoV-2, presented are high power views x400.

Panel A, B: In a kidney from an uninfected control mouse of the same background (C57bl/6J) as the transgenic k18hACE2 mice (**A**) or an infected k18hACE2 mouse that received ACE2 1-618-DDC-ABD (**B**), TUNEL positive staining is absent.

Panels C: Small TUNEL positive bodies (green) were observed in the kidney of an untreated, infected k18hACE2 mouse. In some areas TO-PRO™-3 iodide staining colocalizes with small bodies stained positive for TUNEL. The exact nature of the small TUNEL positive bodies is not clear but may represent DNA fragments after nuclear disintegration (1). Scale bars =20um.

Fig. E9.

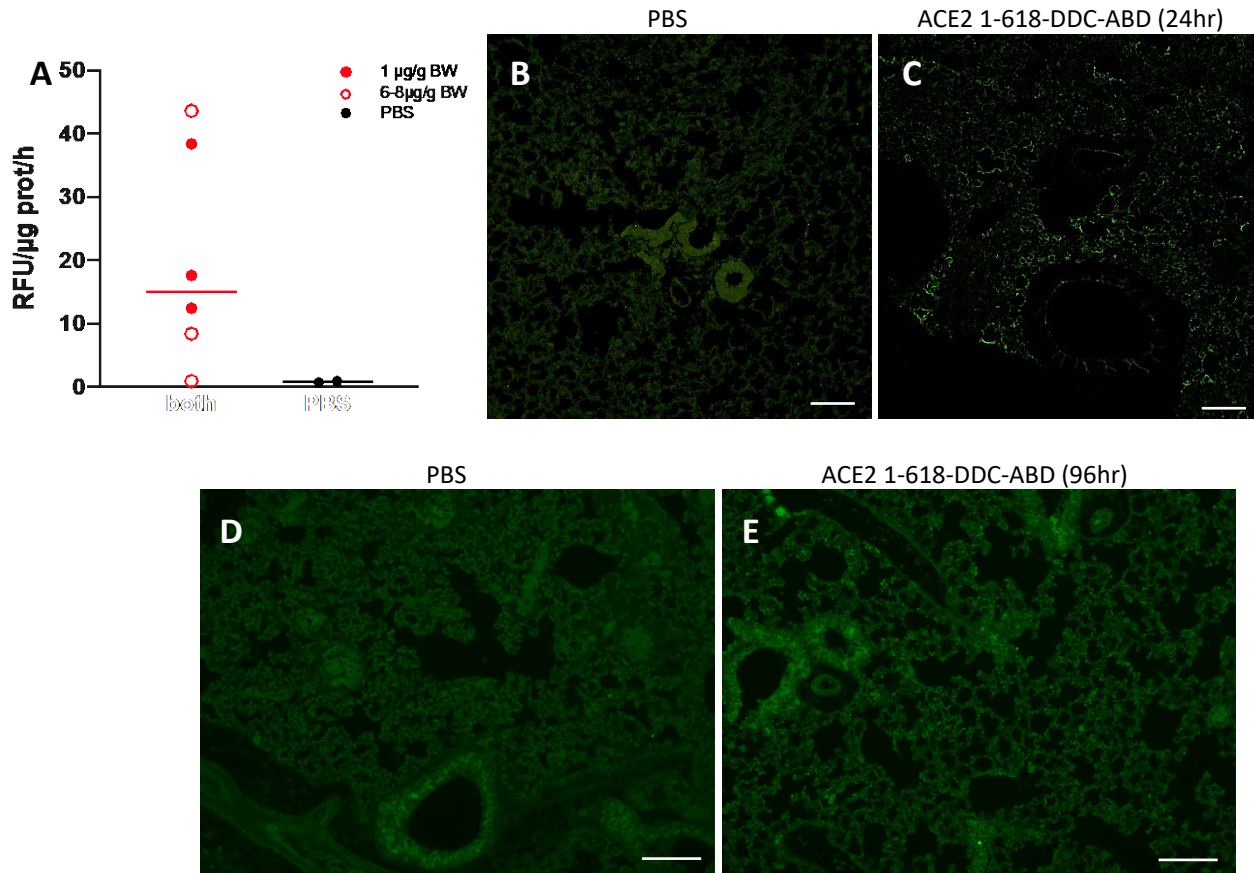


Figure E9. Lung ACE2 activity and staining after intranasal administration of ACE2 1-618-DDC-ABD in controls (A-C) and infected k18hACE2 mice (D, E).

Panel A-C. ACE2 1-618-DDC-ABD (1 or 6-8μg/g BW) or PBS was administered intranasally to uninfected wild-type mice. 24 hours later, lung ACE2 activity (**A**) and staining for ACE2 (**B, C**) was performed. Animals that received ACE2 1-618-DDC-ABD had variable but substantial lung ACE2 activity whereas controls did not (**A**). Staining of the lung with an ACE2 antibody confirmed the presence of ACE2 in alveoli (**C**) compared to a control that received vehicle (PBS) (**B**). Magnification: 200x, scale bar = 100μm.

Panel D. In lungs of an infected, PBS-treated k18hACE2 mouse that was sacrificed 6 days post viral inoculation, ACE2 staining was very weak, scale bar = 100μm.

Panel E. In lungs of an infected k18hACE2 mouse sacrificed also at day 6, that had received its final dose of ACE2 1-618-DDC-ABD 96 hours prior, ACE2 staining was detectable Magnification: 100x, scale bar = 100μm.

Table 1.

Score	Description
0	Pre-inoculation: mice are bright, alert, active, normal fur coat and posture
1	Post-inoculation (PI): mice are bright, alert, active, normal fur coat and posture, no weight loss
1.5	Mice present with slightly ruffled fur but are active, or weight loss might occur but <2.5%, recovery can be expected
2	Ruffled fur or less active or weight loss <5%, recovery might occur
2.5	Ruffled fur or not active but moves when touched or hunched posture or difficulty breathing or weight loss 5-10%, Recovery is unlikely but still might occur
3	Ruffled fur or inactive but moves when touched or difficulty breathing or weight loss at 11-20%, recovery is not expected
4	Ruffled fur or positioned on its side or back or dehydrated or difficulty breathing or weight loss >20% or labored breathing, recovery is not expected
5	death

Table 1. Scoring system in BSL-3 facility for health evaluation of mice infected with SARS-CoV-2.

References:

1. Moore CL, Savenka AV, Basnakian AG. TUNEL Assay: A Powerful Tool for Kidney Injury Evaluation. International Journal of Molecular Sciences. 2021;22(1):412.